MATERIALS CHEMISTRY
FRONTIERS

RESEARCH ARTICLE

View Article Online
View Journal | View Issue

Cite this: *Mater. Chem. Front.*, 2018, **2**, 1568

A supramolecular hyperbranched polymer with multi-responsiveness constructed by pillar[5]arene-based host–guest recognition and its application in the breath figure method†

Yuezhou Liu,[a] Yingyi Zhang,[b] Huangtianzhi Zhu,[a] Hu Wang,[a] Wei Tian *[b] and Bingbing Shi *[a]

Received 9th May 2018,
Accepted 18th June 2018

DOI: 10.1039/c8qm00220g

rsc.li/frontiers-materials

In this work, a disulfide-bridged bispillar[5]arene ($\mathbf{A_2}$) and tritopic neutral guest molecule ($\mathbf{B_3}$) were synthesized and used to construct supramolecular hyperbranched polymers (SHPs) utilizing pillar[5]arene-based host–guest interactions. In particular, a supramolecular gel with interesting reversible gel–sol transition in response to a temperature change and redox owing to the dynamic host–guest complexation and the characteristics of the disulfide bond can be obtained *via* the self-assembly behavior of the SHPs under high concentration. Moreover, honeycomb-patterned films can be successfully prepared by utilizing the breath figure method.

Introduction

Supramolecular polymers, which jointly have the advantages of supramolecular chemistry and polymeric materials, not only own traditional polymeric characteristics, but also possess novel structures and functions, making them exceptional candidates for materials chemistry.[1,2] Moreover, the reversible and tunable nature of noncovalent interactions endows supramolecular polymers with some excellent properties, such as responsiveness to environmental stimuli,[3–5] self-healing,[6–8] recycling[9,10] and degradability.[11,12] Until now, diverse supramolecular polymers have been constructed by noncovalent interactions, such as host–guest interactions,[13–15] hydrogen bonds,[16–19] metal coordination[20] and π–π stacks.[21] Among them, supramolecular hyperbranched polymers (SHPs), which can be constructed through direct and indirect methodologies,[22] have attracted great interest due to their unique chemical and physical properties and potential applications in many fields such as biochemistry[23] and materials science.[24]

Host–guest interactions, as a kind of crucial noncovalent interaction to design supramolecular polymers, exhibit high efficiencies and distinct properties in constructing supramolecular polymer recognition motifs between macrocyclic hosts and the corresponding guests. Pillar[*n*]arenes,[25–35] as an emerging macrocyclic host next to cyclodextrins,[36,37] crown ethers,[38,39] calixarenes[40] and cucurbiturils,[41,42] are composed of *n* hydroquinone units held together by methylene bridges linking the para positions in cyclic arrays. The efficient recognition capabilities and easy functionalization properties endow pillar[*n*]arenes with a wide range of applications in supramolecular polymers,[43,44] drug delivery systems,[45] sensors,[46] green catalysis,[47] and so on. However, the multi-responsive SHPs based on the pillar[*n*]arenes recognition system have rarely been reported. Herein, we constructed a SHP with thermal and redox responsiveness by the host–guest interactions between the disulfide-bridged bispillar[5]arene ($\mathbf{A_2}$) and tritopic neutral guest ($\mathbf{B_3}$) (Scheme 1). It is noteworthy that dithiothreitol (DTT) can reduce the disulfide bond into two thiols quickly *via* an

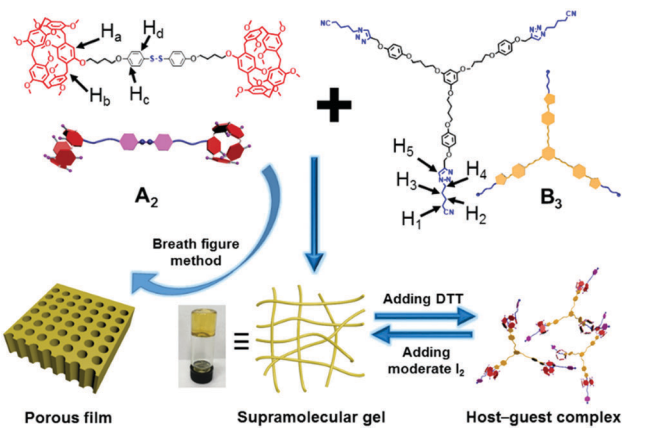

Scheme 1 Chemical structures of $\mathbf{A_2}$ and $\mathbf{B_3}$, and a cartoon representation of the formation of the supramolecular gel and porous film.

[a] *Department of Chemistry, Zhejiang University, Hangzhou 310027, P. R. China. E-mail: bingbingshi@zju.edu.cn*
[b] *Key Laboratory of Space Applied Physics and Chemistry, Ministry of Education and Shaanxi Key Laboratory of Macromolecular Science and Technology, School of Science, Northwestern Polytechnical University, Xi'an 710072, P. R. China. E-mail: happytw_3000@163.com*

† Electronic supplementary information (ESI) available: Synthetic procedures, characterization and other materials. See DOI: 10.1039/c8qm00220g

immediate and mild process, and the regeneration of the disulfide bond can be controlled by the oxidation of iodine (I_2), which endows the SHPs with efficient redox-responsiveness. Meanwhile, the host–guest interactions are quite sensitive to temperature, resulting in the thermal responsiveness of the SHPs. Moreover, the SHPs can self-assemble into a supramolecular gel with reversible gel–sol transition in response to a temperature change and redox under high concentration. Interestingly, the regeneration of the disulfide bond was realized by adding I_2 as an oxidizing agent. After adding moderate I_2 into the sol, an aubergine supramolecular gel was obtained. However, the gel can be transformed into an aubergine solution after the addition of excess I_2. This characteristic is novel in supramolecular chemistry. Furthermore, the SHPs can be used to construct honeycomb-patterned films utilizing the breath figure method, which possesses potential applications in degradable materials by redox due to the characteristic of the disulfide bond. This work will be helpful in designing supramolecular hyperbranched polymers, supramolecular gels and 2D order materials, which may contribute to the development of their application in self-healing materials, absorption and separation.

Results and discussion

Design and synthesis of host molecule A_2 and guest molecule B_3

In a previous report,[48] Yang's group has synthesized a bispillararene connected by a disulfide bond by the oxidation of two thiols. However, this method is relatively tedious to prepare thiol-pillar[5]arene. Here, we constructed disulfide-bridged phenol by the oxidation of 4-hydroxythiophenol with high yield, and then the disulfide-bridged bispillar[5]arene was obtained by the substitution reaction between compound **1** and **2**. On the other hand, Li's group has demonstrated a neutral guest bearing a cyano site and a triazole site at its ends,[49] which is an effective guest for pillar[5]arene with an association constant of 10^4 M^{-1} in the case of an alkylated derivative. In view of this and as a part of our research effort, we prepared neutral guest $\mathbf{B_3}$, which has three cyano sites and triazole sites at the end of the molecule *via* a substitution reaction and click reaction.

Host–guest complexation studies

First, an attempt to study the interaction between the disulfide-bridged bispillar[5]arene $\mathbf{A_2}$ and neutral guest $\mathbf{B_3}$ was carried out by ^{1}H NMR characterization in $CDCl_3$ (Fig. 1). The resulting ^{1}H NMR spectrum showed obvious upfield shifts of the signals of protons H_1, H_2, H_3, H_4 and H_5 from molecule $\mathbf{B_3}$ while the signals of protons of H_a and H_b on $\mathbf{A_2}$ shifted downfield, indicating that the cyanoalkyl groups of $\mathbf{B_3}$ were encapsulated into the cavity of pillararene and further demonstrating the complexation between disulfide-bridged bispillar[5]arene $\mathbf{A_2}$ and neutral guest $\mathbf{B_3}$. In addition, from the 2D NOESY NMR spectrum of the solution of $\mathbf{A_2}$ and $\mathbf{B_3}$, NOE correlation signals were observed between the H_a and H_b protons of bispillar[5]arene $\mathbf{A_2}$ and H_{1-5} of guest molecule $\mathbf{B_3}$, which convincingly verified the formation of the host–guest complex (Fig. S9, ESI†).

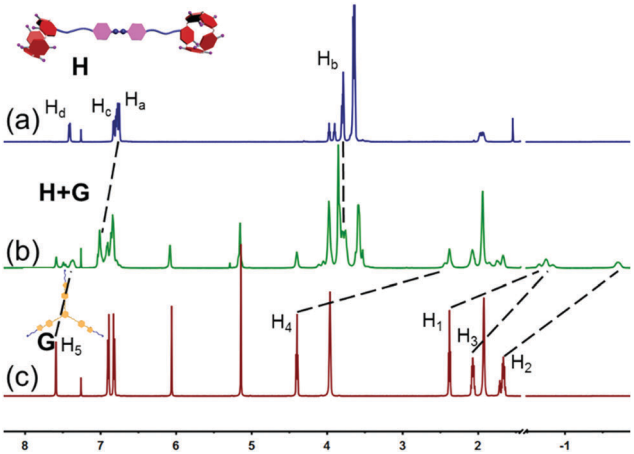

Fig. 1 Partial ^{1}H NMR spectra (600 MHz, 298 K) in $CDCl_3$: (a) 6.00 mM $\mathbf{A_2}$; (b) 6.00 mM $\mathbf{A_2}$ and 4.00 mM $\mathbf{B_3}$; (c) 4.00 mM $\mathbf{B_3}$.

Characterization of the SHPs

A supramolecular hyperbranched polymer was expected to be obtained *via* host–guest interactions in $CHCl_3$. The concentration-dependent ^{1}H NMR spectra of the $\mathbf{A_2}$–$\mathbf{B_3}$ complexes provided vital insights into the self-assembly behavior. As shown in Fig. 2a, the

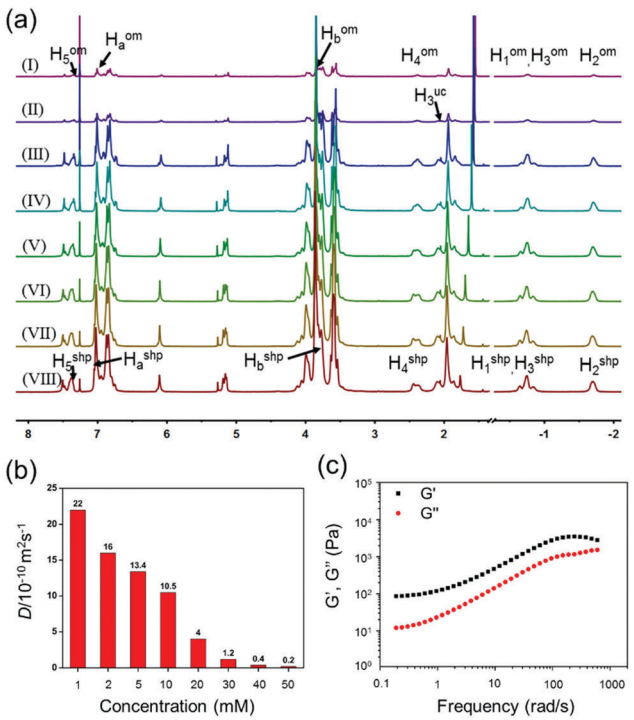

Fig. 2 (a) Partial ^{1}H NMR spectra (600 MHz, $CDCl_3$, 298 K) of mixtures of a 3 : 2 molar ratio of $\mathbf{A_2}$ and $\mathbf{B_3}$ at different concentrations of $\mathbf{A_2}$: (I) 1.00 mM, (II) 2.00 mM, (III) 5.00 mM, (IV) 10.0 mM, (V) 20.0 mM, (VI) 30.0 mM, (VII) 40.0 mM, (VIII) 50.0 mM. Peaks of uncomplexed monomers, oligomers, and supramolecular hyperbranched polymers, are designated as uc, om, and shp, respectively; (b) concentration dependence of the diffusion coefficient D (600 MHz, 298 K) in $CDCl_3$ of mixtures of a 3 : 2 molar ratio of $\mathbf{A_2}$ and $\mathbf{B_3}$ at different $\mathbf{A_2}$ concentrations: 1.00 mM, 2.00 mM, 5.00 mM, 10.0 mM, 20.0 mM, 30.0 mM, 40.0 mM, 50.0 mM; (c) rheological results of the supramolecular gel constructed by 75.0 mM $\mathbf{A_2}$ and 50.0 mM $\mathbf{B_3}$ in $CHCl_3$.

^{1}H NMR spectra of the $\mathbf{A_2}$–$\mathbf{B_3}$ complexes at concentrations of $\mathbf{A_2}$ in the range of 1.00–50.0 mM were tanglesome due to the slow-exchange host–guest interactions on the NMR time scale. At a low concentration of $\mathbf{A_2}$ (1.00 mM), the signals of protons H_4 and H_3 were split into two sets of peaks, corresponding to complexed branched oligomers (H_{4om} and H_{3om}) and uncomplexed molecules (H_{3uc}), proving the slow-exchange binding between $\mathbf{A_2}$ and $\mathbf{B_3}$. With the monomer concentration increasing, the signals of protons H_1, H_2 and H_3 of the cyanoalkyl groups shifted downfield. In addition, all of the main peaks broadened markedly, which gave clear evidence for the formation of supramolecular polymers.

In addition, 2D diffusion-ordered ^{1}H NMR spectroscopy (DOSY) experiments were performed to provide straightforward evidence for the formation of SHPs. As shown in Fig. 2b, the measured weight-average diffusion coefficient D values of the $\mathbf{A_2}$–$\mathbf{B_3}$ complexes decreased from 22.0×10^{-10} m^2 s^{-1} to 0.2×10^{-10} m^2 s^{-1} with an increase in the concentration of $\mathbf{A_2}$ (with 2/3 equiv. $\mathbf{B_3}$) from 1.00 mM to 50.0 mM, indicating that the high-molecular-weight polymeric species were successfully formed. Interestingly, a yellowish transparent supramolecular gel can be obtained upon increasing the concentration of the monomers (75.0 mM $\mathbf{A_2}$ and 50.0 mM $\mathbf{B_3}$).

The characterization of the supramolecular gel

Rheological characterization is an important analytical tool to characterize the supramolecular gel because it can display the material properties directly. Therefore, an oscillatory sweep experiment was carried out to obtain the rheological properties of the supramolecular gel (75 mM $\mathbf{A_2}$ with 2/3 equiv. $\mathbf{B_3}$, Fig. 2c). The result of the rheological experiment showed the frequency dependence of the storage modulus G' and loss modulus G'' of the supramolecular gel, and G' was larger than G'' over a wide frequency range of 0.1–100 rad s^{-1}, indicating that the supramolecular gel was stable. Moreover, the morphology of the supramolecular gel was characterized by transmission electron microscopy (TEM) and scanning electron microscopy (SEM). As shown in Fig. 3, a three-dimensional network structure could be observed clearly.

Supramolecular gels that can exhibit a response to external stimuli are always attractive. It's well known that host–guest interactions are quite sensitive to temperature. The temperature-variant NMR experiments of $\mathbf{A_2}$–$\mathbf{B_3}$ complexes showed the reduction of the intensity of the peaks of H_1, H_2, and H_3 along with the increase of temperature from 298 K to 328 K (Fig. S16, ESI†), which indicated that the host–guest interaction decreased. Therefore, as shown in Fig. 4a, heating and cooling can result in a reversible gel–sol transition. The disulfide bond has gained extensive attention because of its biological activities and potential reactivity.[50] Furthermore, the cleavage and formation of the disulfide bond can be controlled by redox. To examine the redox-responsiveness of compound $\mathbf{A_2}$ in more detail, cyclic voltammetry was conducted in a solution of tetrabutylammonium hexafluorophosphate (0.10 mM in $CHCl_3$) (Fig. S17a, ESI†). Obvious peaks in the cyclic voltammetry curves were observed, which indicated that the cleavage and formation of the disulfide bond can be controlled by redox. Moreover, DTT, as one of the most used reductants, was

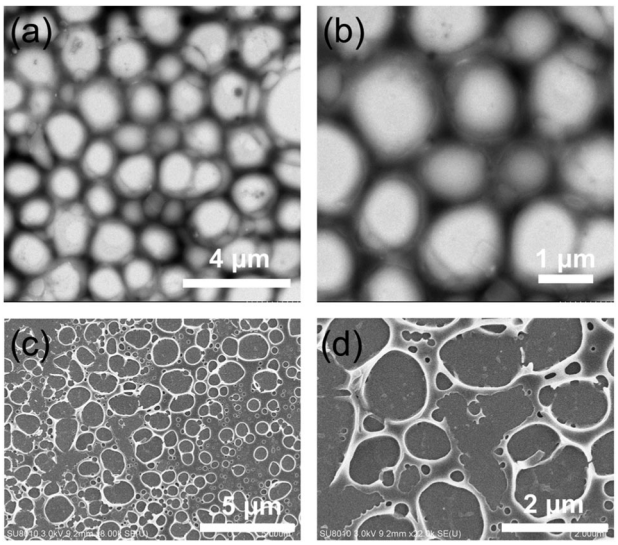

Fig. 3 (a), (b) TEM images and (c), (d) SEM images of the supramolecular polymer network of the mixtures of a 3 : 2 molar ratio of $\mathbf{A_2}$ and $\mathbf{B_3}$ at 20.0 mM of $\mathbf{A_2}$.

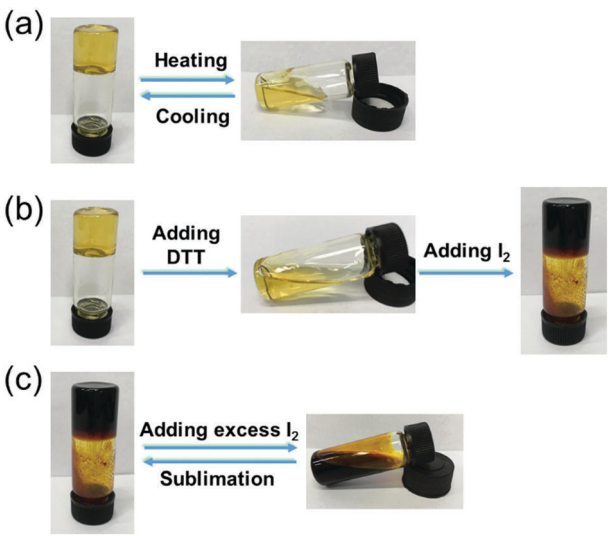

Fig. 4 The gel–sol transitions of the supramolecular gel triggered by (a) heating and cooling, (b) redox, and (c) adding excess I_2 and sublimation.

selected to reduce the disulfide bonds under mild conditions. As shown in Fig. 4b, upon the addition of 1.00 equiv. of DTT into the supramolecular gel, the gel gradually collapsed within 2 hours, resulting in a gel–sol transition. Furthermore, I_2 is widely used for disulfide bond formation reactions with a rapid rate and high yield in peptide synthesis. Therefore, here we chose I_2 as an oxidizing agent to realize the regeneration of the disulfide bond. Upon the addition of moderate I_2 into the sol, an aubergine supramolecular gel was ultimately obtained within 4 hours. Interestingly, after adding excess I_2 into the aubergine supramolecular gel, the gel was destroyed and transformed into an aubergine solution. According to the previous work, I_2 can locate in the cavity of pillar[5]arene which destroyed the host–guest

interaction between pillar[5]arene and the guest molecule.[46,51] ^{1}H NMR study was further used to investigate the mechanism in $CDCl_3$ (Fig. S17b, ESI†). The DMP5 was selected as a model host molecule, and the ^{1}H NMR spectra of DMP5 and DMP5 with excess I_2 are shown in Fig. S17b (ESI†). The resulting ^{1}H NMR spectra showed that the signals of the protons on DMP5 shifted downfield, indicating the existence of the interactions between the pillararene and I_2, which could hinder the host–guest interaction between pillararene and other guest molecules. Moreover, the aubergine solution could be transformed into a supramolecular gel by sublimation in air, which endowed the material with reversible stimuli-responsiveness (Fig. 4c).

Honeycomb-patterned films fabricated by the breath figure method

Inspired by the three-dimensional network structure of SHPs (Fig. 3), the obtained SHPs were tested to determine whether they could be used to fabricate potential topological supramolecular materials such as 2D honeycomb-patterned films, which have potential applications in the fields of separation,[52] drug release[53] and catalysis.[54] As shown in Fig. 5, an ordered honeycomb film was prepared using the breath figure method. A 7.5 wt% concentration of SHPs in $CHCl_3$ was used to prepare the honeycomb-patterned structure, the average pore diameter of which was about 1.0–1.5 μm by SEM analysis. Above all, the disulfide bond can be destroyed by the addition of DTT. Therefore, DTT can be used to control the formation of the honeycomb-patterned films. After adding 1.0 equiv. DTT into the solution of SHPs (7.5 wt%) in $CHCl_3$, irregular particles were formed (Fig. 5c and d). This is direct evidence that the honeycomb-patterned films were fabricated based on SHPs instead of small molecules, and this characteristic endows the honeycomb-patterned films with degradable properties.

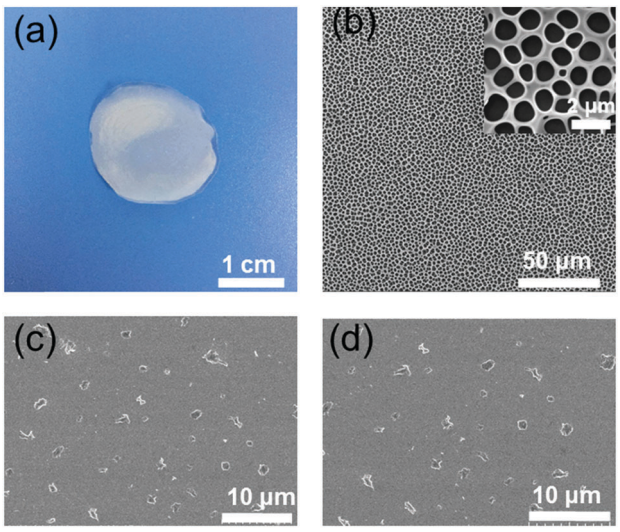

Fig. 5 (a) Digital photo of the honeycomb-patterned films made from a solution of $\mathbf{A_2}$–$\mathbf{B_3}$ complexes in $CHCl_3$ at the concentration of 7.5 wt% using the BF method; (b) SEM of the honeycomb-patterned films. (c and d) SEM images of films made from a solution of $\mathbf{A_2}$–$\mathbf{B_3}$ complexes in $CHCl_3$ at the concentration of 7.5 wt% after adding 1.0 equiv. DTT using the BF method.

Conclusions

In summary, we have designed and synthesized a disulfide-bridged bispillar[5]arene $\mathbf{A_2}$ and a tritopic neutral guest molecule $\mathbf{B_3}$, which can self-assemble into supramolecular hyprebranched polymers, and the supramolecular hyprebranched polymers can form a supramolecular gel at a high concentration of the monomers based on the host–guest interactions between pillar[5]arenes and the neutral guests. The supramolecular polymer gel possessed multi-responsiveness and the reversible gel–sol transitions of the supramolecular gel can be triggered by heating, cooling, redox, adding excess I_2 and sublimation, which can facilitate its application as a smart material. Moreover, the resulting SHPs can be employed to prepare honeycomb-patterned films using the breath figure method. Furthermore, the honeycomb-patterned films have potential applications in degradable materials by redox due to the characteristic of the disulfide bond. This work will be helpful in designing supramolecular hyperbranched polymers, supramolecular gels and 2D ordered materials, which may contribute to the development of their applications in self-healing materials, absorption and separation.

Experimental

Materials and instrumentation

All reagents were commercially available and used as supplied without further purification. Compounds **1**,[55] **2**,[56] **3**,[57] and **6**[31] were synthesized according to the previous work. ^{1}H NMR spectra, ^{13}C NMR, NOESY and DOSY NMR spectra were recorded with an Agilent DD2-600 with the use of the deuterated solvent as the lock and the residual solvent or TMS as the internal reference. Scanning electron microscopy investigations were carried out on a JEOL 6390LV instrument. SEM samples were prepared *via* the vacuum freeze-drying methodology. Transmission electron microscopic investigations were carried out on a HITACHI HT-7700 instrument. High-resolution mass spectrometric experiments were performed using a Bruker 7 Tesla FT-ICR mass spectrometer equipped with an electrospray source (Billerica, MA, USA). The disc-shaped gels with thickness of 1 mm and diameter of 20 mm were adhered to the plates and surrounded by silicone oil. Frequency sweeps were performed on the samples with a strain amplitude of 0.05%.

Synthesis of $\mathbf{A_2}$

The synthetic route of $\mathbf{A_2}$ is shown in the Scheme S1 (ESI†). A mixture of compound **1** (1.00 g, 1.41 mmol), **2** (0.14 g, 0.56 mmol), and K_2CO_3 (0.78 g, 0.56 mmol) in CH_3CN (75 mL) was stirred at reflux for 48 hours. After the solid was filtered off, the solvent was concentrated by rotary evaporation. The crude product was dissolved in CH_2Cl_2 (100 mL) and washed three times with H_2O (50 mL). The organic layer was dried over anhydrous Na_2SO_4 and concentrated to afford a jacinth solid, which was further purified by

column chromatography using ethyl acetate/petroleum ether (1 : 2). The fractions containing the product were concentrated to give $\mathbf{A_2}$ as a white solid (0.63 g, 68%). The ^{1}H NMR spectrum of $\mathbf{A_2}$ is shown in Fig. S1 (ESI†). ^{1}H NMR spectrum of $\mathbf{A_2}$ (600 MHz, 298 K) in $CDCl_3$ δ (ppm): 7.40–7.42 (d, J = 12 Hz, 4H), 6.82–6.83 (d, J = 6 Hz, 4H), 6.75–6.77 (m, 20H), 3.96–3.99 (t, J = 6 Hz, 4H), 3.89–3.91 (t, J = 6 Hz, 4H), 3.79–3.81 (m, 20H), 3.63–3.66 (m, 54H), 1.98 (m, 8H). The ^{13}C NMR spectrum of $\mathbf{A_2}$ is shown in Fig. S2 (ESI†). ^{13}C NMR spectrum of $\mathbf{A_2}$ (150 MHz, 298 K) in $CDCl_3$ δ (ppm): 159.5, 151.0, 150.1, 132.8, 128.5, 115.2, 114.2, 68.1, 67.8, 56.0, 29.9, 26.3. HR ESI-MS: m/z calcd for $[M + H^+]$ $C_{108}H_{119}O_{22}S_2^+$, 1831.76; found 1831.77, error 5 ppm.

Synthesis of compound 4

The synthetic route of $\mathbf{B_3}$ is shown in the Scheme S2 (ESI†). A solution of compound **3** (5.29 g, 10.0 mmol), compound **5** (5.28 g, 40.0 mmol) and K_2CO_3 (13.8 g, 100 mmol) in CH_3CN (250 mL) was stirred at reflux for 48 hours. After the solid was filtered off, the mixture was evaporated to afford the crude product, which was isolated by flash column chromatography using ethyl acetate/petroleum ether (1 : 10) to give **4** as a white solid (7.25 g, 78%). The ^{1}H NMR spectrum of **4** is shown in Fig. S4 (ESI†). ^{1}H NMR spectrum of 4 (600 MHz, 298 K) in $CDCl_3$ δ (ppm): 6.76–6.86 (m, 12H), 5.99 (s, 3H), 4.56 (d, J = 6 Hz, 6H), 3.90 (s, 12H), 2.43 (t, J = 3 Hz, 3H), 1.87 (m, 12H). The ^{13}C NMR spectrum of 4 is shown in Fig. S5 (ESI†). ^{13}C NMR spectrum of 4 (150 MHz, 298 K) in $CDCl_3$ δ (ppm): 159.8, 152.8, 150.6, 115.1, 114.3, 92.8, 77.9, 74.3, 66.9, 55.6, 25.0.

Synthesis of guest molecule B_3

A solution of compound **4** (6.60 g, 9.0 mmol), compound **6** (5.1 g, 41.1 mmol), $CuSO_4{\cdot}5H_2O$ (2.27 g, 9.0 mmol) and sodium ascorbate (2.67 g, 18 mmol) in 80 mL DMF was stirred at 90 °C for 24 hours. After the reaction finished, the crude product was dissolved in CH_2Cl_2 (400 mL) and washed three times with H_2O (200 mL). The organic layer was dried over anhydrous Na_2SO_4 and concentrated to afford a grayish yellow solid, which was further purified by recrystallization in moderate CH_3CN (5.35 g, 54%). The ^{1}H NMR spectrum of $\mathbf{B_3}$ is shown in Fig. S7 (ESI†). ^{1}H NMR spectrum of $\mathbf{B_3}$ (600 MHz, 298 K) in $CDCl_3$ δ (ppm): 7.59 (s, 3 H), 6.81–6.90 (m, 12H), 6.06 (s, 3H), 5.14 (s, 3H), 6.22 (t, J = 6 Hz, 3H), 3.96 (s, 12H), 2.39 (t, J = 6 Hz, 6H), 2.09 (m, 6H), 1.92 (s, 12H), 5.99 (m, 6H). The ^{13}C NMR spectrum of $\mathbf{B_3}$ is shown in Fig. S8 (ESI†). ^{13}C NMR spectrum of $\mathbf{B_3}$ (150 MHz, 298 K) in $CDCl_3$ δ (ppm): 160.9, 153.7, 152.4, 144.9, 122.7, 119.0, 116.0, 115.6, 94.1, 68.1, 67.6, 62.8, 49.3, 29.1, 26.2, 26.0, 22.4, 16.8. HR ESI-MS: m/z calcd for $[2M + H^+ + K^+]$ $C_{120}H_{145}N_{24}O_{18}K^{2+}$, 1124.54; found 1124.51, error −3 ppm.

Fabrication of honeycomb-patterned films by the breath figure method

A mixture of a 3 : 2 molar ratio of $\mathbf{A_2}$ and $\mathbf{B_3}$ was dissolved in chloroform to obtain a solution of SHPs at a concentration of 7.5 wt%. Next, about 50 μL of the polymer solution was dripped on the treated PET substrate by a syringe. During this process, a steady airflow of moist nitrogen was maintained through the surface of the polymer solution. The temperature could be decreased due to the evaporation of chloroform, which resulted in the condensation of water vapor on the surface of the solution. Subsequently, chloroform and water was evaporated conjointly, and an ordered porous structure was finally formed on the cover of the polymer membrane.

Conflicts of interest

There are no conflicts to declare.

Acknowledgements

This work was supported by the Fundamental Research Funds for the Central Universities.

Notes and references

1 T. F. A. De. Greef, M. M. J. Smulders, M. Wolffs, A. P. H. J. Schenning, R. P. Sijbesma and E. W. Meijer, *Chem. Rev.*, 2009, **109**, 5687.
2 S. Dong, B. Zheng, F. Wang and F. Huang, *Acc. Chem. Res.*, 2014, **47**, 1982.
3 R. J. Wojtecki, M. A. Meador and S. J. Rowan, *Nat. Mater.*, 2011, **10**, 14.
4 X. Ma and H. Tian, *Acc. Chem. Res.*, 2014, **47**, 1971.
5 W. Xia, M. Ni, C. Yao, X. Wang, D. Chen, C. Lin, X.-Y. Hu and L. Wang, *Macromolecules*, 2015, **48**, 4403.
6 A. Phadke, C. Zhang, B. Arman, C.-C. Hsu, R. A. Mashelkar, A. K. Lele, M. J. Tauber, G. Arya and S. Varghese, *Proc. Natl. Acad. Sci. U. S. A.*, 2012, **109**, 4383.
7 J. W. Steed, *Chem. Soc. Rev.*, 2010, **39**, 3686.
8 T. Kakuta, Y. Takashima, M. Nakahata, M. Otsubo, H. Yamaguchi and A. Harada, *Adv. Mater.*, 2013, **25**, 2849.
9 X. Li, J. Fei, Y. Xu, D. Li, T. Yuan, G. Li, C. Wang and J. Li, *Angew. Chem., Int. Ed.*, 2018, **57**, 1903.
10 M. Abbasi, *J. Chin. Chem. Soc.*, 2017, **64**, 896.
11 Y. Kohsaka, K. Nakazono, Y. Koyama, S. Asai and T. Takata, *Angew. Chem., Int. Ed.*, 2011, **50**, 4872.
12 Q. Wang, M. Cheng, L. Tian, Q. Fan and J. Jiang, *Polym. Chem.*, 2017, **8**, 6058.
13 A. Harada, Y. Takashima and M. Nakahata, *Acc. Chem. Res.*, 2014, **47**, 2128.
14 H. Yang, B. Yuan and X. Zhang, *Acc. Chem. Res.*, 2014, **47**, 2106.
15 G. Yu, Z. Yang, X. Fu, B. C. Yung, J. Yang, Z. Mao, L. Shao, B. Hua, Y. Liu, F. Zhang, Q. Fan, S. Wang, O. Jacobson, A. Jin, C. Gao, X. Tang, F. Huang and X. Chen, *Nat. Commun.*, 2018, **9**, 766.
16 T. Park and S. C. Zimmerman, *J. Am. Chem. Soc.*, 2006, **128**, 13986.
17 Y. Ma, S. V. Kolotuchi and S. C. Zimmerman, *J. Am. Chem. Soc.*, 2002, **124**, 13757.
18 X. Yan, Z. Liu, Q. Zhang, J. Lopez, H. Wang, H.-C. Wu, S. Niu, H. Yan, S. Wang, T. Lei, J. Li, D. Qi, P. Huang,

J. Huang, Y. Zhang, Y. Wang, G. Li, J. B.-H. Tok, X. Chen and Z. Bao, *J. Am. Chem. Soc.*, 2018, **140**, 5280.
19 Z. Gao, Y. Han, S. Chen, Z. Li, H. Tong and F. Wang, *ACS Macro Lett.*, 2017, **6**, 541.
20 F. Peng, G. Li, X. Liu, S. Wu and Z. Tong, *J. Am. Chem. Soc.*, 2008, **130**, 16166.
21 I. Welterlich and B. Tieke, *Macromolecules*, 2011, **44**, 4194.
22 W. Tian, X. Li and J. Wang, *Chem. Commun.*, 2017, **53**, 2531.
23 G. Fernández, E. M. Pérez, L. Sánche and N. Martín, *J. Am. Chem. Soc.*, 2008, **130**, 2410.
24 R. Gu, J. Yao, X. Fu, W. Zhou and D.-H. Qu, *Chem. Commun.*, 2015, **51**, 5429.
25 T. Ogoshi, S. Kanai, S. Fujinami, T. A. Yamagishi and Y. Nakamoto, *J. Am. Chem. Soc.*, 2008, **130**, 5022.
26 D. Cao, Y. Kou, J. Liang, Z. Chen, L. Wang and H. Meier, *Angew. Chem., Int. Ed.*, 2009, **48**, 9721.
27 T. Ogoshi, H. Kayama, D. Yamafuji, T. Aoki and T. Yamagishi, *Chem. Sci.*, 2012, **3**, 3221.
28 X.-F. Ji, D.-Y. Xia, X. Yan, H. Wang and F.-H. Huang, *Acta Polym. Sin.*, 2017, 9–18.
29 X.-B. Hu, L. Chen, W. Si, Y. Yu and J.-L. Hou, *Chem. Commun.*, 2011, **47**, 4694.
30 Y.-M. Zhang, B. Shi, H. Li, W.-J. Qu, G.-Y. Gao, Q. Lin, H. Yao and T.-B. Wei, *Polym. Chem.*, 2014, **5**, 4722.
31 Y. Liu, L. Shangguan, H. Wang, D. Xia and B. Shi, *Polym. Chem.*, 2017, **8**, 3783.
32 X. Liao, L. Guo, J. Chang, S. Liu, M. Xie and G. Chen, *Macromol. Rapid Commun.*, 2015, **36**, 1492.
33 G. Yu, J. Yang, X. Fu, Z. Wang, L. Shao, Z. Mao, Y. Liu, Z. Yang, F. Zhang, W. Fan, J. Song, Z. Zhou, C. Gao, F. Huang and X. Chen, *Mater. Horiz.*, 2018, **5**, 429.
34 J.-F. Chen, Q. Lin, Y.-M. Zhang, H. Yao and T.-B. Wei, *Chem. Commun.*, 2017, **53**, 13296.
35 J.-F. Chen, Q. Lin, H. Yao, Y.-M. Zhang and T.-B. Wei, *Mater. Chem. Front.*, 2018, **2**, 999.
36 J. Liu, G. Chen, M. Guo and M. Jiang, *Macromolecules*, 2010, **43**, 8086.
37 Z.-X. Zhang, X. Liu, F. J. Xu, X. J. Loh, E.-T. Kang, K.-G. Neoh and J. Li, *Macromolecules*, 2008, **41**, 5967.
38 N. Yamaguchi and H. W. Gibson, *Angew. Chem., Int. Ed.*, 1999, **38**, 143.
39 H. W. Gibson, Y. X. Shen, M. C. Bheda and C. Gong, *Polymer*, 2014, **55**, 3202.
40 D.-S. Guo and Y. Liu, *Chem. Soc. Rev.*, 2012, **41**, 5907.
41 K. Kim, *Chem. Soc. Rev.*, 2002, **31**, 96.
42 S. Ghosh and L. Isaacs, *J. Am. Chem. Soc.*, 2010, **132**, 4445.
43 B. Shi, D. Xia and Y. Yao, *Chem. Commun.*, 2014, **50**, 13932.
44 Z. Zhang, Y. Luo, J. Chen, S. Dong, Y. Yu, Z. Ma and F. Huang, *Angew. Chem., Int. Ed.*, 2011, **50**, 1397.
45 Q. Duan, Y. Cao, Y. Li, X. Hu, T. Xiao, C. Lin, Y. Pan and L. Wang, *J. Am. Chem. Soc.*, 2013, **135**, 10542.
46 Q. Lin, K.-P. Zhong, J.-H. Zhu, L. Ding, J.-X. Su, H. Yao, T.-B. Wei and Y.-M. Zhang, *Macromolecules*, 2017, **50**, 7863.
47 Y. Liu, B. Lou, L. Shangguan, J. Cai, H. Zhu and B. Shi, *Macromolecules*, 2018, **51**, 1351.
48 C.-L. Sun, J.-F. Xu, Y.-Z. Chen, L.-Y. Niu, L.-Z. Wu, C.-H. Tung and Q.-Z. Yang, *Polym. Chem.*, 2016, **7**, 2057.
49 C. Li, K. Han, J. Li, Y. Zhang, W. Chen, Y. Yu and X. Jia, *Chem. – Eur. J.*, 2013, **19**, 11892.
50 R. Singh and G. M. Whitesides, *J. Am. Chem. Soc.*, 1990, **112**, 1190.
51 K. Jie, Y. Zhou, E. Li, Z. Li, R. Zhao and F. Huang, *J. Am. Chem. Soc.*, 2017, **139**, 15320.
52 J. Zhang, Z. Meng, J. Liu, C. Schlaich, Z. Yu and X. Deng, *J. Mater. Chem. A*, 2017, **5**, 16369.
53 Y. Su, J. Dang, H. Zhang, Y. Zhang and W. Tian, *Langmuir*, 2017, **33**, 7393.
54 L. Zhang, L. Chen, S.-X. Liu, J. Gong, Q. Tang and Z.-M. Su, *Dalton Trans.*, 2018, **47**, 105.
55 L. Liu, D. Cao, Y. Jin, H. Tao, Y. Kou and H. Meier, *Org. Biomol. Chem.*, 2011, **9**, 7007.
56 F. Vibert, S. R. A. Marque, E. Bloch, S. Queyroy, M. P. Bertrand, S. Gastaldi and E. Besson, *Chem. Sci.*, 2014, **5**, 4716.
57 H. Yang, Z. Ma, Z. Wang and X. Zhang, *Polym. Chem.*, 2014, **5**, 1471.